Histol Histopathol (2023) 38: 1205-1217

Histology and Histopathology
From Cell Biology to Tissue Engineering

ORIGINAL ARTICLE Open Access

Circ-0000979 promotes the development of gastric carcinoma by sponging miR-136 and modulating SP1 mRNA expression level

Lihua Zhang[1]*, Fengjuan Xing[2]* and Lei Bao[2]

[1]Department of Pathology, Fourth Medical Center of PLA General Hospital, Beijing and [2]Department of Pathology, The Affliated Yantai Yuhuangding Hospital of Qingdao University, Yantai, Shangdong province, PR China

*Co-first author: Lihua Zhang, Fengjuan Xing

Summary. Circular RNAs (circRNAs) are a new class of non-coding RNAs that play pivotal biological roles in several types of cancer cells. However, the role of circ-0000979 in gastric cancer (GC) has never been explored. Therefore, the current study aims to examine the functional effects of circ-0000979 in GC development and progression. The expression level of circ-0000979 was validated using qRT-PCR analysis. We found that circ-0000979 is significantly upregulated in GC samples. Using AGS and HGC27 GC cell line, we examined the biological functions and regulatory mechanisms of circ-0000979 in GC *in vitro* and *in vivo* by knocking down circ-0000979. We found that circ-0000979 is subcellularly localized in the cytoplasm of GC cells. Functionally, silencing circ-0000979 leads to a significant reduction in GC cell proliferation and migration. *In vivo* assays showed that circ-0000979 knockdown markedly reduced GC tumor growth. CircRNA interactome predicted miR-136 as circ-0000979 targeting miRNA, while starbase prediction result showed that miR-136 targeted the 3'UTR region of SP1 mRNA. Taken together, our results demonstrated that circ-0000979, as a carcinogenic circRNA, promotes the progression of GC by regulating the miR-136/SP1 pathway. Circ-0000979 is a potential RNA-based therapeutic target for GC treatment.

Key words: CircRNA, Circ-0000979, Gastric carcinoma, miR-136, SP1

Corresponding Author: Lei Bao, Department of Pathology, The Affliated Yantai Yuhuangding Hospital of Qingdao University, No. 20, Yuhuangding East Road, Yantai, 264000, Shangdong province, China. e-mail: bl258538751@163.com

www.hh.um.es. DOI: 10.14670/HH-18-578

Introduction

Gastric cancer (GC) continues to rank top among the most common malignancies across the world. It is the third leading cause of cancer-related death across the globe after lung cancer and colorectal cancer (Bray et al., 2018). Its pathogenesis can be attributed to several factors, including environmental e.g dietary habits and social behavior, and genetic factors like the diffuse hereditary GC, where mutations in the nucleotide sequence of E-cadherin gene being reported as a predisposition factor (Machlowska et al., 2020; Martin-Richard et al. 2020). Epidemiological study has shown that the mortality rate of GC in China ranks third in the world, making the search for effective treatment inevitable (Rawla and Barsouk, 2019). Currently, gastroscopy is being used for the detection and diagnosis of GC (Cho et al., 2020; Zhu et al., 2020). However, most cases are detected only at a later stage. In addition, a more efficient and non-invasive method is needed to detect tumors early. Besides, surgical resection remains the most widely used method for GC treatment, but the high recurrence rate of the disease, and its low 5-year survival rate continues to pose a threat to its effective treatment and management (D'Angelica et al., 2004; Katai et al., 2018; Sitarz et al., 2018). Therefore, it is imperative to further understand the pathogenesis of GC in order to seek new and more effective early diagnosis and treatment methods.

In recent years, many studies have shown that abnormal expression of circRNA in tissues is strongly associated with a variety of human diseases (Jin et al., 2019; Li et al., 2020; Peng et al., 2020). In cancer, many studies have proved that circRNA regulates tumor progression and can be used as a diagnostic marker (Tang et al., 2018; Zong et al., 2018). As an example, overexpression of circRNA_102171 has been reported to promote the progression of papillary thyroid cancer (PTC) by activating the Wnt/β-catenin pathway in a

CTNNBIP1-dependent manner (Bi et al., 2018). In particular, low expression of hsa_circRNA_001587 (circRNA0000979) promotes proliferation, migration, invasion, and angiogenesis in pancreatic cancer (PC) cells by regulating the miR-223/SLC4A4 axis (Zhang et al., 2020). However, there have been no reports of its involvement in the pathogenesis and progression of GC. Through computational analysis, we found that hsa-circ-0000979 can target miR-136 in many cancers. MiR-136 has been reported to play an important role in inhibiting tumor development (Zheng et al., 2017; Yu et al., 2018; Qu et al., 2019). Yu et al revealed the therapeutic potential of miR-136 in GC as it was found to effectively promote apoptosis in GC cells by targeting AEG-1 and BCL2 gene (Yu et al., 2018). Therefore, understanding the relationship between hsa-circ-0000979 and miR-136 in the regulation of GC progression can provide adequate information for the development of effective GC therapeutics. The SP1 gene is a transcription factor protein that has been reported to regulate multiple cancer-related genes (Shi and Zhang, 2019). It has been reported to be highly expressed in GC tumors and be closely related to the prognosis of GC (Tian et al., 2020; Zang et al., 2020).

With the understanding of the potential biological functions of the aforementioned molecules in GC cells and their probable molecular mechanisms, a series of *in vivo* and *in vitro* experiments was designed to investigate the underlying relationship among hsa-circ-0000979, miR-136, and SP1 genes in GC cells, with the hope of uncovering a novel therapeutic target for GC therapy. Our results show that circ-0000979 involvement in the progression of GC is due to its targeted adsorption of miR-136, which in turn regulates the expression of SP1. To our knowledge, this study is the first to report the expression, function, and mechanism of circ-0000979 in GC. Circ-0000979 could be a novel therapeutic target for the treatment of GC.

Materials and methods

Patient samples

GC tissues and the adjacent ones were collected from 52 patients who had not undergone preoperative chemotherapy or radiotherapy at the The 960th Hospital of PLA and were labeled and stored at -80°C. Tumor-node metastasis (TNM) staging system, UICC (Union for International Cancer Control) criteria was used to make the diagnosis. This study was approved by the Ethical Committee of The 960th Hospital of PLA.

Bioinformatics analysis

The expression profile of circ RNA in the 52 GC tissues and the adjacent tissues were obtained from the Gene Expression Omnibus database (GEO) with the accession number GSE78092. The limma package R software (version 3.4.1) was employed to visualize (heat map analysis and volcano plot) the differentially expressed circ RNA between the GC and the adjacent tissues.

Target Gene Prediction

Prediction of Circ-0000979 target miRNA (miR-136) was performed with circRNA interactome (https://circinteractome.nia.nih.gov/). StarBase v2.0 (http://starbase.sysu.edu.cn/) was employed to predict the miRNAs target 3'UTR region of mRNA (SP1).

Cell culture

Normal gastric epithelial cells (GSE-1) and GC cell lines (AGS, HGC27, MKN-45, MKN74) were cultured in Dulbecco's Modified Eagle's Medium-High Glucose (90%, DMEM-H; Gibco, USA) augmented with 10% fetal bovine serum (FBS; Thermo Scientific, USA). Human gastric epithelial cells (GSE-1), human embryonic kidney cells (HEK 293T) and human GC cells (HGC-27) were cultured in 90% RPMI-1640 and 90% RPMI-1640 (w/o HEPES, Gibco, USA) with 10% FBS supplementation. In addition, cell lines were procured from BeNa Culture Collection (BNCC, China) and kept under an atmosphere of 37°C and 5% CO_2.

Cell Transfection

ShRNA (sh-circ#1, sh-circ#2) specific to human circ-0000979, miR-136 mimics and inhibitor, negative control sequences (sh-NC and miR-NC) were created by Gene-Pharma (China). Cells were cultured to 40-60% density in a 6-well plate, and transfected with Lipofectamine 2000 (Invitrogen, CA, USA). After 48h of cell transfection, cells were obtained to confirm the efficacy of the transfection and the functional experiments.

RNase R treatment and qRT-PCR

Total RNA from cell lines and tissues was isolated with TRIzol reagent (Life Technologies, USA) using RNeasy Mini Kit (QIAGEN, China), and were reversely transcribed into complementary DNA (cDNA) with AMV reverse transcription kit (TaKaRa, Japan) Then, RNase R treatment, genomic DNA (gDNA) was extracted with QIAamp DNA Mini Kit (QIAGEN, China). Quantitative real-time PCR (qRT-PCR) was performed using the SYBR Premix Ex TaqTM kit (TaKaRa, Japan). CircRNA and miRNA expressions were normalised to the levels of GAPDH and U6 and estimated with the $2^{-\Delta\Delta Ct}$ method.

Cytoplasm and nuclear Localization of circ-0000979

The NE-PER™ Cytoplasmic and Nuclear Extraction Reagents Kit (ThermoFisher Scientific, USA) was used

to confirm the cytoplasmic localization of circ-0000979 in AGS cells. In accordance with the manufacturer's guide, the AGS nuclear and cytoplasmic constituents were sorted and collected. Quantitative real time (qRT)-PCR was employed to estimate the expression of circ-0000979 in the cell nucleus and cytoplasm. GAPDH and U6 were used as the cytoplasm and nucleus localization control respectively.

Cell counting Kit-8 (CCK-8) assay

Inoculation of cells was done in a 96-well plate with 2×10^3 cells/well. At 24, 48, and 72h, absorbance at 450 nm of each sample was determined with the CCK-8 kit (Dojindo Laboratories, Japan) for plotting the viability curves.

Colony formation assay

For the colony formation assays, the transfected cells were trypsinised and plated in 6-well plates. Routine incubation was done for 10 days at 37°C. Colonies were then fixed with methanol for 10 minutes and dyed with crystal violet (0.1%) for 15 minutes. Cell colonies were counted and then analysed.

Transwell assay

A total of 5×10^5 cells/ mL was used to prepare the cell suspension. Approximately, 200 μL of suspension and 700 μL of medium containing FBS (20%, Thermo Scientific, USA) was added on the upper and lower of the transwell chamber respectively and cultured for 48h. Migratory cells in the lower chamber were induced using methanol (Sigma-Aldrich) for 15 min, crystal violet (0.2%) for 20 min and acquired with a microscope (Nikon, USA). At random, five fields per sample were chosen for counting and capturing of cells. Similarly, invasion assay was performed in a transwell insert pre-coated with Matrigel.

RNA immunoprecipitation

RNA immunoprecipitation (RIP) assays were done with a Magna RIP Kit (Millipore, USA) following the manufacturer′s protocol. Briefly, miR-136 mimics and control were transfected into HGC-27 and AGS cells. A total of 2×10^7 HGC-27 and AGC cells were lysed in RIP lysis buffer (100 μL) complemented with protease inhibitor (Roche, USA) and RNase inhibitor (Promega, USA) cocktail. After treatment with DNase I (Roche, USA), the lysate was diluted using RIP immuno-precipitation buffer (900 μL) and incubated with antibody-coupled magnetic beads (anti-AGO2, Abcam, USA), and approximately 10 μL of RNA immuno-precipitation mixture was saved as input. Afterward, beads were washed using RIP wash buffer six times and treated using proteinase K for 30 minutes at 37°C.

Western blot

After cell lysis using radioimmunoprecipitation assay (RIPA; Beyotime, China) on ice for 15 min, and centrifugation of the mixture at 14000×g for 15 min at 4°C. Bicinchoninic acid (BCA, Pierce, USA) method was employed to estimate the cellular protein concentration. Equal amounts of protein samples were separated on SDS-PAGE, and loaded on PVDF membrane (Millipore, USA) and blocked using skim milk (5%). Then, incubation using primary antibody E-cadherin (1:1000; Abcam, USA), N-cadherin (1:1000; Abcam, USA), Vimentin (1:1000; Abcam, USA), SNAIL (1:1000; Abcam, USA) and GAPDH as an endogenous control was performed overnight at 4°C and then secondary antibody (HRP-conjugated; Abcam, USA) incubation for 1h at room temperature was done, followed by the visualization of the immunoreactive bands with an enhanced chemiluminescence kit (Millipore, USA). All presented data were based on biological triplicates.

Luciferase reporter assay

The circ-0000979 with miR-136 binding sites were generated and sub-cloned into a pGL2-Base vector (Promega, USA). HEK-293T cells were placed into 96-well plates and were co-transfected with firefly luciferase reporter mixture, pRL-CMV Renilla luciferase reporter, SP1 and miR-136 mimics with Lipofectamine 2000 (Invitrogen, USA). After incubation for 48 hr, the activities of the firefly and Renilla luciferase activities were measured using a dual luciferase reporter assay system (Promega, USA). The activity of the Renilla luciferase was taken as the internal control.

Biotinylated RNA Pull-down Assay

Biotinylated miR-136 mimics and miR-NC were synthesised by RiboBio (China). The firmly expressed circ-0000979 GC cells were transfected with 50 nM of biotinylated miR-136 mimics or miR-NC with Lipofectamine RNAiMax (Life Technologies, USA), collected after transfection for 48h and sonication followed. Retain aliquots (50 μL) of the cell lysate for input and incubate the remaining cell lysate at 4°C for 3h while using C-1 magnetic beads (Life Technologies, USA) and washing by wash buffer. The collected RNAs were cleansed using RNeasy Mini Kit (QIAGEN, China) for RT-PCR.

In-vivo assays for tumor growth

To study tumor growth using *in vivo* technique, a xenograft model was developed using 6 to 8-week-old nude mice (Shanghai Laboratory Animal Center, China). Suspended transfected cells ($1x10^3$) with sh-NC, sh-circ#1 and sh-circ#2 were inoculated into each mouse

subcutaneously. Tumour growth was assessed every 7 days, and tumour volumes were estimated (0.5 × length × width). After inoculation, mice were sacrificed, and tumors were excised and weighed. All experiments were approved by the Ethical Committee of The 960th Hospital of PLA.

Statistical analysis

GraphPad Prism (Version 6.0) was employed for the statistical analyses, all data were recorded as means ± standard deviation. One-way ANOVA or student′s t test were used to determine the statistical significance for the comparison of two or more groups with $P<0.05$, and Pearson correlation was used for association between two groups. All experiments were performed in triplicate.

Results

Circ-0000979 is upregulated in the GC tissue samples and cell lines.

GEO: GSE78092 microarray data show differential expression of circRNAs, including circ-0000979, in the GC tissue data compared to the adjacent normal tissue samples after filtration (|log2FC|>1, *P* value<0.05) (Fig. 1a). Similarly, volcano plot shows that circRNAs were significantly upregulated and downregulated in the gastric cancer sample respectively (Fig. 1b). The expression level of circ-0000979 was further verified in GC tissues collected from patients after surgical resection through qRT-PCR. Results confirm that circ-0000979 is significantly upregulated in the 52 GC tissues when compared to the adjacent normal tissues, suggesting that circ-0000979 might play a significant role in the pathogenesis and progression of GC ($p<0.01$, Fig. 1c). Furthermore, the overall survival curve of the GC patients in the current study was plotted using Kaplan-Meier method with log rank test. The median expression value of circ-0000979 calculated after dividing the 52 GC patient group into a high expression and low expression group was used for the KM plot. Our results show that GC patients with high circ-0000979 expression level had a much poorer prognosis than those with low circ-0000979 expression (Fig. 1d). We also analyzed the relationship between the expression level of circ-0000979 and various clinicopathological features observed among the GC patients included in this study. As shown in Table 1, the expression of circ-0000979 significantly correlated with GC staging, grade, and lymph node metastasis, but had no significant correlation with the gender and age of the GC patients ($p<0.05$). For further molecular experiment, GC cell lines were tested for the circ-0000979 expression which was significantly higher in the GC cell lines (AGS, HGC27, MKN-45, MKN74) than in the normal gastric epithelial cells (GSE-1). Notably, AGS and HGC27 had the highest expression of circ-0000979, thus, they were employed in researching the molecular function of circ-0000979 in GC and its regulatory mechanism (Fig. 1e). To confirm the circular structure of circ-0000979, AGS cell line was treated with Mock and Rnase R separately, after which the expression of GADPH and circ-0000979 was quantified through qRT-PCR analysis. Conspicuously, the expression of GADPH was drastically reduced after Rnase R treatment compared to Mock treatment, while no significant difference was observed in the expression level of circ-0000979 after both Mock and Rnase R treatment, indicating the circular nature of circ-0000979 ($p<0.01$, Fig. 1f). Besides, we found that circ-0000979 is mostly localized in the cytoplasm of GC cell lines as evidenced in the significantly higher circ-0000979-fold change observed in the cytoplasmic fraction relative to nuclear fraction ($p<0.01$, Fig. 1g).

Knockdown of circ-0000979 represses GC cell proliferation and metastasis in vitro

To further elucidate the biological function of circ-0000979, two interfering RNAs targeting circ-0000979 were constructed into pLKO.1-puro expression vector and then transfected into AGS and HGC27 cell lines for stable knockdown of circ-0000979. After, qRT-PCR was used to assess the knockdown efficiency. Results show that sh-circ-0000979 significantly knocked down more than 50% of circ-0000979 in the cell lines ($p<0.01$, Fig. 2a). Furthermore, the effect of circ-0000979 knockdown on GC cell proliferation and migration was assessed through CCK-8 assay, colony formation assay, and transwell assay. As shown in Fig. 2b, silencing circ-0000979 resulted in a significant reduction in the viability of the AGS and HGC27 GC cell lines when compared to the control group ($p<0.01$). Colony

Table 1. Clinicopathological data of GC patients in the current study.

Clinicopathological characteristics	Total	High expression	Low expression	χ^2	*p* value
Gender					
male	33	18	15	0.664	0.415
female	23	10	13		
Age□year□					
≤60	30	16	14	0.287	0.592
>60	26	12	14		
Histological grade					
Low	26	10	20	7.179	0.007
Middle+High	30	18	8		
Lymph node metastasis					
Positive	31	19	11	4.595	0.032
Negative	25	9	17		
TMN stages					
I +II	30	13	17	1.149	0.284
III+ IV	26	15	11		
Distant metastasis					
M0	22	7	15	4.791	0.029
M1	34	21	13		

formation assay shows that both sh-circ#1 and sh-circ#2 markedly reduced the number of colonies formed in the AGS and HGC27 GC cell lines, while transwell assay result also confirmed that circ-0000979 knockdown could significantly reduce the migration ability of the GC cell lines ($p<0.01$, Fig. 2c,d). Western blot analysis revealed that circ-0000979 knockdown markedly increased the protein expression level of E-cadherin but repressed the expression of N-cadherin, vimentin, and snail protein in AGS and HGC27 cells (Fig. 2e).

Knockdown of circ-0000979 represses development of glioma in vivo

Furthermore, we examined the silencing effect of sh-circ#1 on the progression of GC *in vivo*, using a mouse

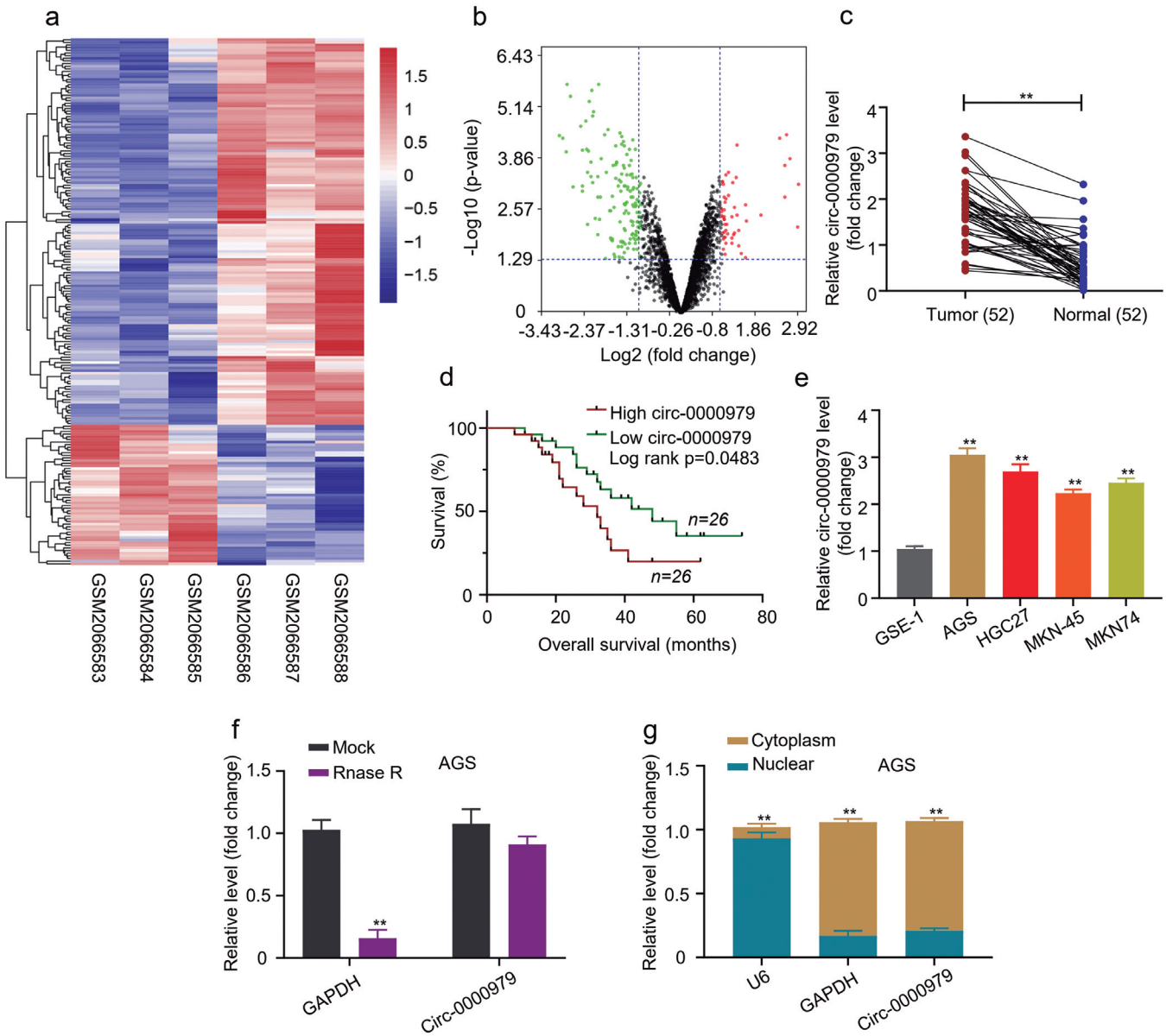

Fig. 1. Circ-0000979 is upregulated in the GC tissue samples and cell lines. **a.** HeatMap showing the differential expression of circRNAs in GC tissue data (GSE78092). **b.** Volcano plot of upregulated and downregulated circRNAs in the GC tissue data. **c.** circ-0000979 expression level in GC tissues confirmed through qRT-PCR. Circ-0000979 was significantly upregulated in the 52 GC tissues resected from GC patients when compared to the adjacent normal tissues. **d.** KM plot shows that GC patients with high circ-0000979 expression level had a much poorer prognosis than those with low circ-0000979 expression. **e.** QRT-PCR analysis of circ-0000979 expression level in different GC cell lines. AGS and HGC27 had the highest expression of circ-0000979. **f.** QRT-PCR confirmatory analysis of the circ-0000979 circular structure in AGS cell line after treatment with Mock and Rnase R. **g.** QRT-PCR analysis revealed that circ-0000979 has a significantly higher circ-0000979-fold change in the cytoplasmic fraction relative to nuclear fraction and is mostly localized in the cytoplasm of GC cell lines. All experiments were performed in triplicates. $^{**}p<0.05$ was chosen as the significant level.

model. The cells with the stably silenced circ-0000979 were subcutaneously inoculated into the right thighs of the nude mice, and these mice were monitored closely for tumor growth for 35 days. As shown in Fig. 3a, GC tumor size was significantly reduced in mice treated with sh-circ#1 compared to those treated with the negative control shRNA (sh-NC). Results show that sh-circ#1 knockdown significantly reduced tumor volume after 35 days of injection, compared to sh-NC (p<0.01, Fig. 3b). Similarly, we found that circ-0000979 knockdown resulted in a significant reduction in tumor weight when compared to the control experiment, implying that silencing circ-0000979 could significantly reduce the progression of GC (p<0.01, Fig. 3c).

Circ-0000979 sponges miR-136 and accelerates it degradation

Bioinformatics prediction of circ-0000979 target miRNA was conducted through the circRNA interactome platform (https://circinteractome.nia.nih.gov/). Results show the presence of a potential binding site between the circ-0000979 and miR-136 seed region which could result in target adsorption of mir-136 by circ-0000979 (Fig. 4a). Dual-luciferase reporter assay shows that the overexpression of mir-36 can significantly inhibit the

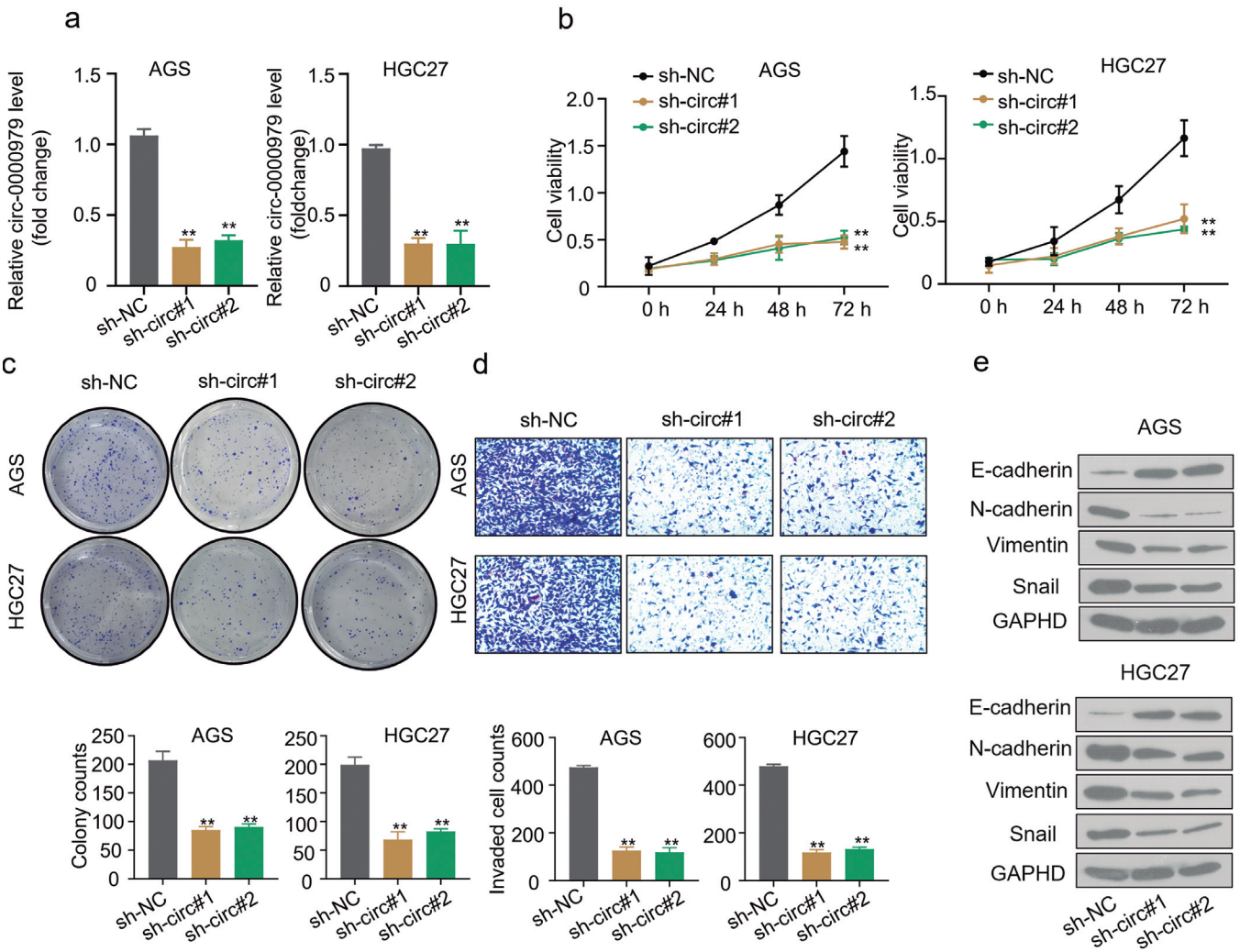

Fig. 2. Knockdown of circ-0000979 represses GC cell proliferation and metastasis *in vitro*. **a.** QRT-PCR analysis of stably circ-0000979 knockdown cell line confirms the effectiveness of the knockdown experiment. Sh-circ-0000979 significantly reduced circ-0000979 expression in the cell lines. **b.** CCK-8 assay shows that silencing circ-0000979 resulted in a significant reduction in the viability of the AGS and HGC27 GC cell lines when compared to the control group. **c.** Colony formation assay shows that both sh-circ#1 and sh-circ#2 markedly reduced the number of colonies formed in the AGS and HGC27 GC cell lines. **d.** Transwell assay result confirms that circ-0000979 knockdown could significantly reduce GC cell migration. **e.** Western blot analysis revealed that circ-0000979 knockdown markedly increased the protein expression level of E-cadherin but repressed the expression of N-cadherin, vimentin, and snail protein in AGS and HGC27 cells. All experiments were performed in triplicate. **p<0.05 was chosen as the significant level.

expression of luciferin in HEK-293T cells transfected with the circ-0000979 wild-type (Wt) sequence reporter gene, however, there was almost no difference in luciferin expression in HEK-293T cells transfected with the circ-0000979 mutant-type (Mut) sequence ($p<0.01$, Fig. 4b). Biotinylated RNA pull-down assay was conducted to further confirm the binding potential of circ-0000979 and mir-136 in the AGS and HGC27 cell lines. The results revealed that the circ-0000979-probe pulled down more miR-136 in both GC cell lines than the Oligo-probe ($p<0.01$, Fig. 4c). Interestingly, we found that circ-0000979 knockdown led to a significant upregulation of mir-136 in both AGS and HGC27 cell lines compared to the control sh-NC knockdown group ($p<0.01$, Fig. 4d). Through qRT-PCR analysis, we examined the expression level of mir-136 in GC tumor cells extracted from patients and found that mir-136 is markedly downregulated in GC patients ($p<0.01$, Fig. 4e). Finally, correlation analysis shows that the expression of mir-136 in GC is negatively correlated with that of circ-0000979 ($p<0.01$, Fig. 4f).

SP1 is the target gene of mir-136

Furthermore, mir-136 target mRNA was also computationally predicted through StarBase v2.0 (http://starbase.sysu.edu.cn/). The results revealed that miR-136 might repress the expression of SP1 gene by binding to the 3'UTR region of its mRNA sequence (Fig. 5a). This was confirmed through dual-luciferase reported assay which revealed the effect of overexpressing mir-136 in HEK-293T cell lines transfected with SP1 reporter gene sequence. We observed that mir-136 overexpression resulted in a significant inhibition of the luciferase activity of the cell lines transfected with SP1 wild-type (Wt) sequence, while no significant inhibition was observed in the luciferase activity of the cell lines transfected with the SP1 mutant-type (Wt) sequence ($p<0.01$, Fig. 5b). QRT-PCR shows that the circ-0000979 knockdown led to a significant reduction in the relative expression of SP1 mRNA in both GC cell lines ($p<0.01$, Fig. 5c). RNA-pulldown assay for Ago2 in the AGS and HGC27 cell lines shows that more mir-136 and SP1 mRNA were significantly enriched in the retrieved Ago2 RNA relative to that of IgG, suggesting the ability of both RNA molecules to bind through to the Ago2 protein complex ($p<0.01$, Fig. 5d). Besides, miR-136 inhibition significantly increased the expression level of SP1 mRNA in the GC cell lines ($p<0.01$, Fig. 5e). Further, qRT-PCR analysis of tumor samples revealed an upregulated expression level of SP1 RNA in GC samples compared to the adjacent normal ones ($p<0.01$, Fig. 5f). Also, Pearson's analysis showed that SP1 mRNA expression level was negatively correlated to that of miR-136 ($p<0.01$, Fig. 5g).

Circ-0000979 promotes proliferation and metastasis of gastric carcinoma by sponging miR-136 and modulating SP1.

To verify the regulatory effect of circ-0000979 on SP1 expression and the resulting effect on cell death, to assess the effects of various cellular phenotypes (such as proliferation and metastasis) on GC progression, miR-136 was inhibited in stable circ-0000979 knockdown cell, while SP1 was overexpressed by an overexpression (oe) plasmid. First, the relative expression level of SP1 mRNA was measured after transfection of the knockdown cell through qRT-PCR analysis. The result shows a significant reduction in the expression of SP1 mRNA in the circ-0000979-knockdown group compared to the sh-NC control group, while miR-136 inhibition and SP1 overexpression significantly restored such expression in both GC cell lines ($p<0.01$, Fig. 6a). The SP1 protein expression level was also assessed after each aforementioned treatment using western blot analysis.

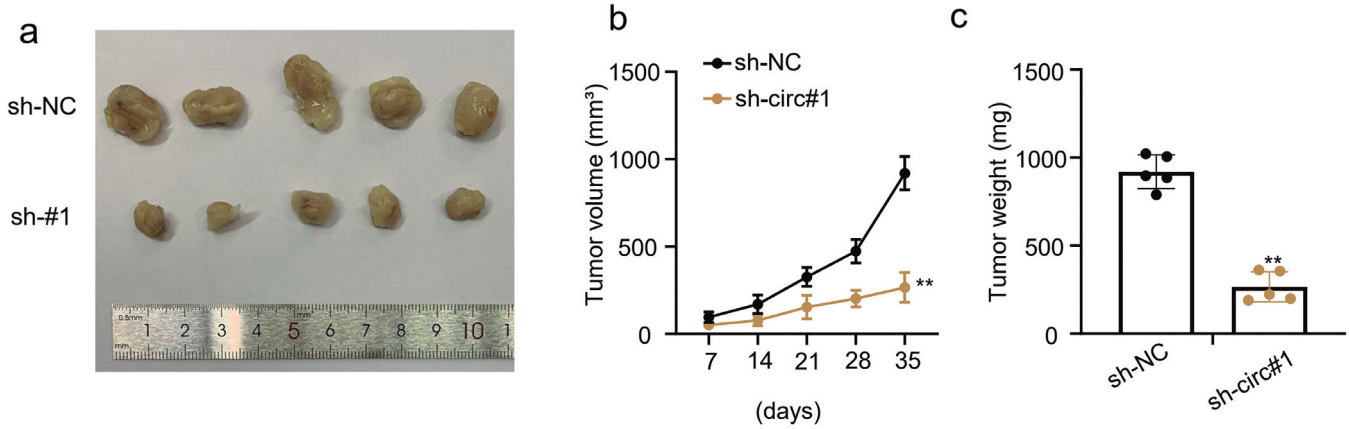

Fig. 3. Knockdown of circ-0000979 represses development of glioma *in vivo*. **a.** An *In vivo* experiment using a mouse model shows that GC tumor size was significantly reduced in models treated with sh-circ#1 compared to those treated with the negative control shRNA (sh-NC). **b.** sh-circ#1 knockdown significantly reduced tumor volume after 35 days of injection, compared to sh-NC. **c.** Circ-0000979 knockdown resulted in a significant reduction in tumor weight when compared to the control experiment. All experiments were performed in triplicate. ** $p<0.05$ was chosen as the significant level.

We found that co-transfecting circ-0000979-knockdown GC cell line with miR-136 inhibitor and SP1 overexpression plasmid (oe-SP1) markedly restored the reduced SP1 protein expression level observed after circ-0000979 knockdown (Fig. 6b). CCK-8 assay revealed that both miR-136 inhibition and overexpressing SP1 significantly increased the GC cell line viability when compared to the viability observed in the circ-0000979-knockdown cell group ($p<0.01$, Fig. 6c). Similarly, through a colony formation assay, we demonstrated that

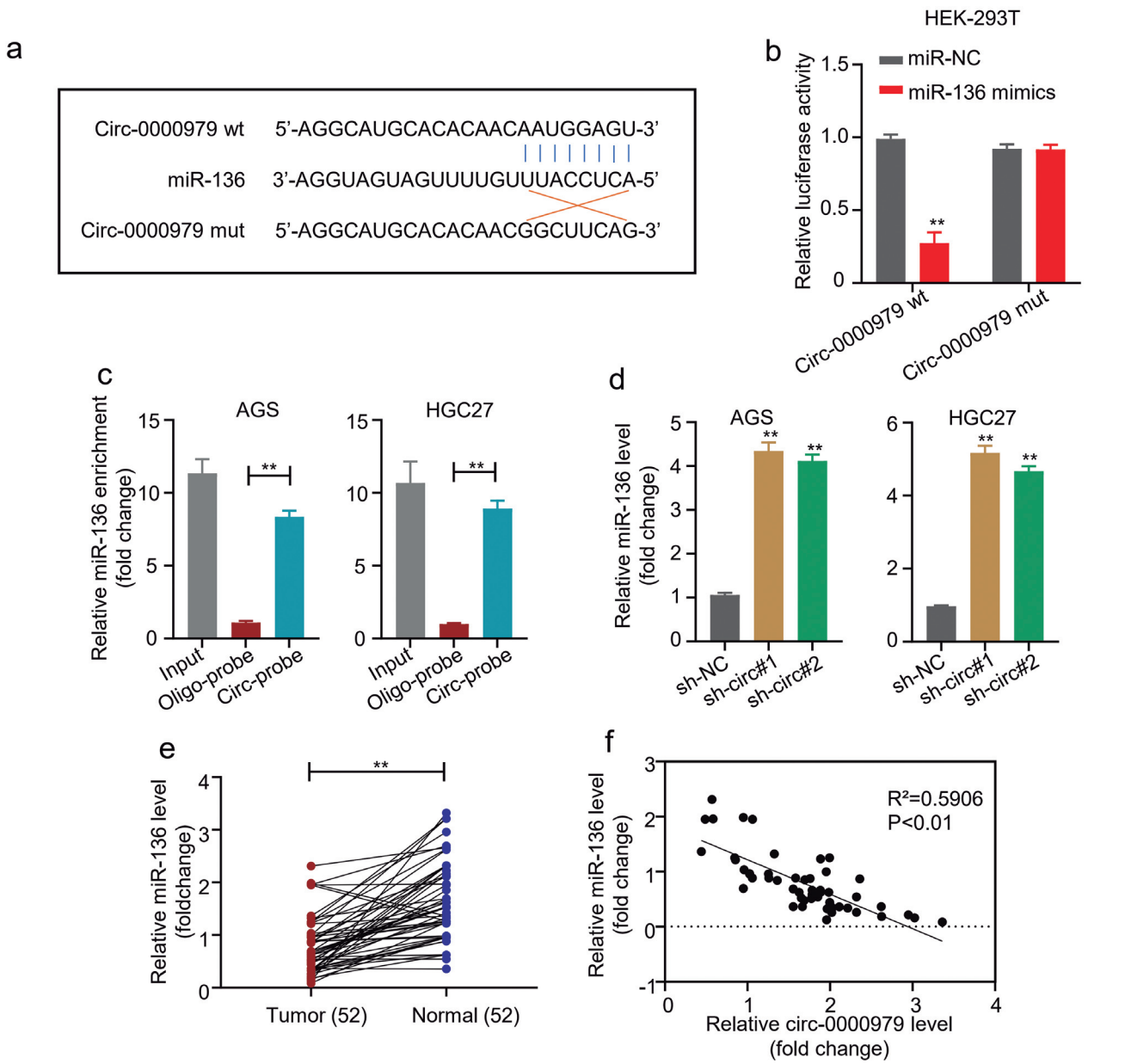

Fig. 4. Circ-0000979 sponges miR-136 and accelerates its degradation. **a.** Bioinformatics prediction using circRNA interactome shows the presence of a potential binding site between the circ-0000979 and miR-136 seed region. **b.** Dual-luciferase reporter assay shows that the overexpression of mir-36 significantly inhibited the expression of luciferin in HEK-293T cells transfected with the circ-0000979 wild-type (Wt) sequence reporter gene but had no significant effect on those transfected with the circ-0000979 mutant-type (Mut) sequence. **c.** Biotinylated RNA pull-down assay revealed that the Circ-0000979-probe pull-down more mir-136 in both GC cell lines compared to the Oligo-probe. **d.** QRT-PCR analysis shows that circ-0000979 knockdown significantly upregulated mir-136 expression level in both AGS and HGC27 cell lines compared to the control sh-NC knockdown group. **e.** QRT-PCR analysis revealed that the expression level of mir-136 in resected tumors was markedly downregulated in GC patients. **f.** Pearson correlation analysis shows that the expression of mir-136 in GC is negatively correlated with that of circ-0000979. All experiments were performed in triplicate. $^{**}p<0.05$ was chosen as the significant level.

inhibiting miR-136 and overexpressing SP1 was able to restore the proliferative ability of GC cell lines (p<0.01, Fig. 6d). Besides, transwell assay result shows that the migration of the stably silenced circ-0000979 GC cell lines significantly increased after co-transfection with either miR-136 inhibitor or SP1 overexpression plasmid (p<0.01, Fig. 6e). Through western blot analysis, we also found that miR-136 inhibition and SP1 overexpression markedly repressed the protein expression level of E-cadherin but increased the expression of N-cadherin, vimentin, and snail protein in the AGS and HGC27 cell lines (Fig. 6f).

Discussion

The importance of circRNA as a major player in tumorigenesis and development has continually been revealed by several researchers (Suzuki and Tsukahara, 2014). Recently, as research that explores the role and mechanism of circRNAs has progressed, knowledge of the function and relationships between circRNAs and human diseases are being elucidated (Fang et al., 2019). Either Upregulated or downregulated, it has been posited to be a novel specific therapeutic target for Gastric Cancer (GC) cells with diverse metastasis ability and

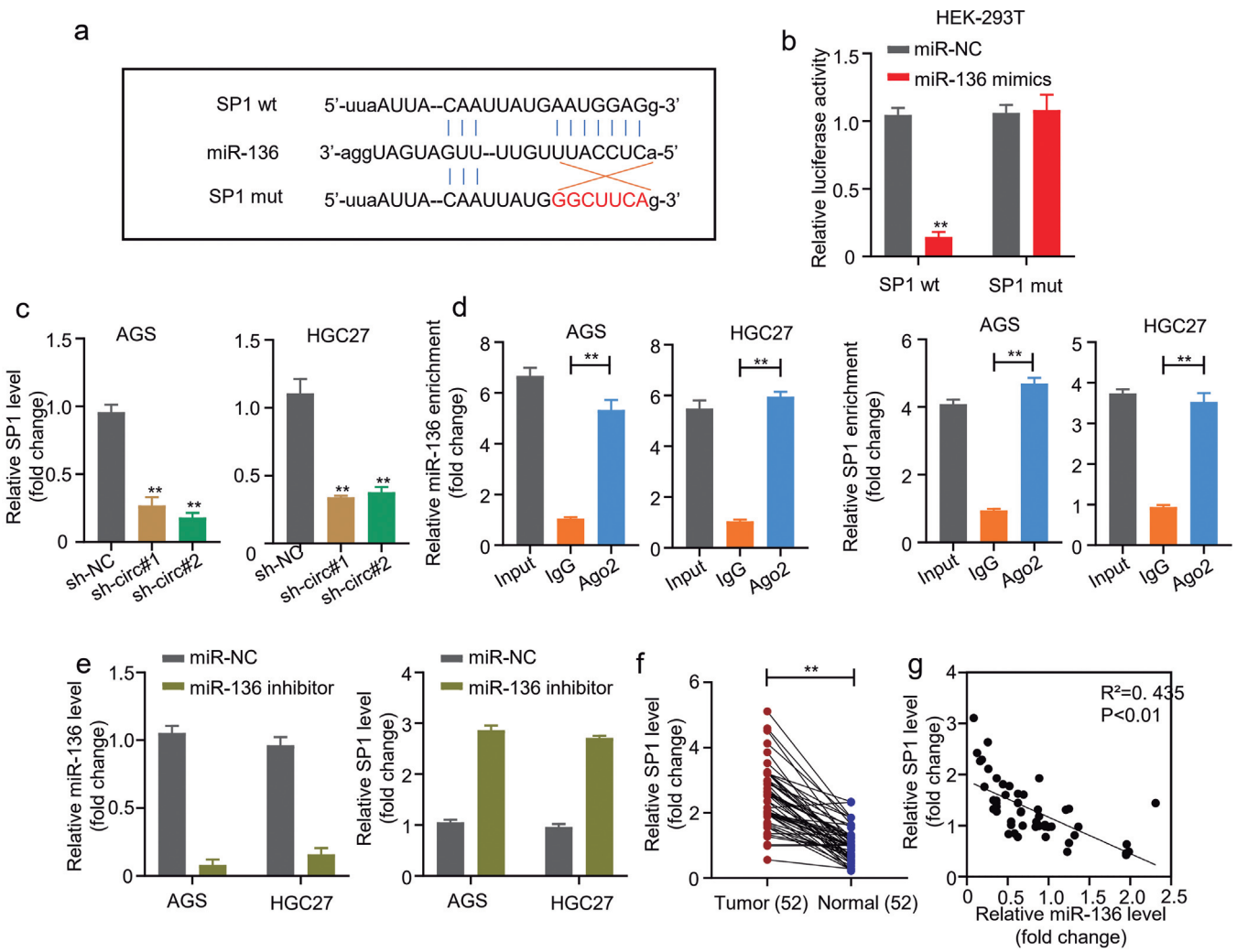

Fig. 5. SP1 is the target gene of mir-136. **a.** Bioinformatics prediction mir-136 target mRNA using StarBase v2.0 revealed that miR-136 might repress the expression of SP1 gene by binding to the 3'UTR region of its mRNA sequence. **b.** Dual-luciferase reporter assay shows that mir-136 overexpression resulted in a significant inhibition of the luciferase activity of the cell lines transfected with SP1 wild-type (Wt) sequence while no significant inhibition was observed in the luciferase activity of the cell lines transfected with the SP1 mutant-type (Wt) sequence. **c.** QRT-PCR shows that circ-0000979 knockdown significantly reduced the relative expression of SP1 mRNA in both GC cell lines. **d.** RNA-pulldown assay shows that more mir-136 and SP1 mRNA were significantly enriched in retrieved Ago2 RNA relative to that of IgG. **e.** QRT-PCR analysis revealed that miR-136 inhibition significantly increased the expression level of SP1 mRNA in the GC cell lines. **f.** QRT-PCR analysis of tumor samples revealed an upregulated expression level of SP1 RNA in GC samples compared to the adjacent normal ones. **g.** Pearson correlation analysis showed that SP1 mRNA expression level was negatively correlated to that of miR-136. All experiments were performed in triplicate. **p<0.05 was chosen as the significant level.

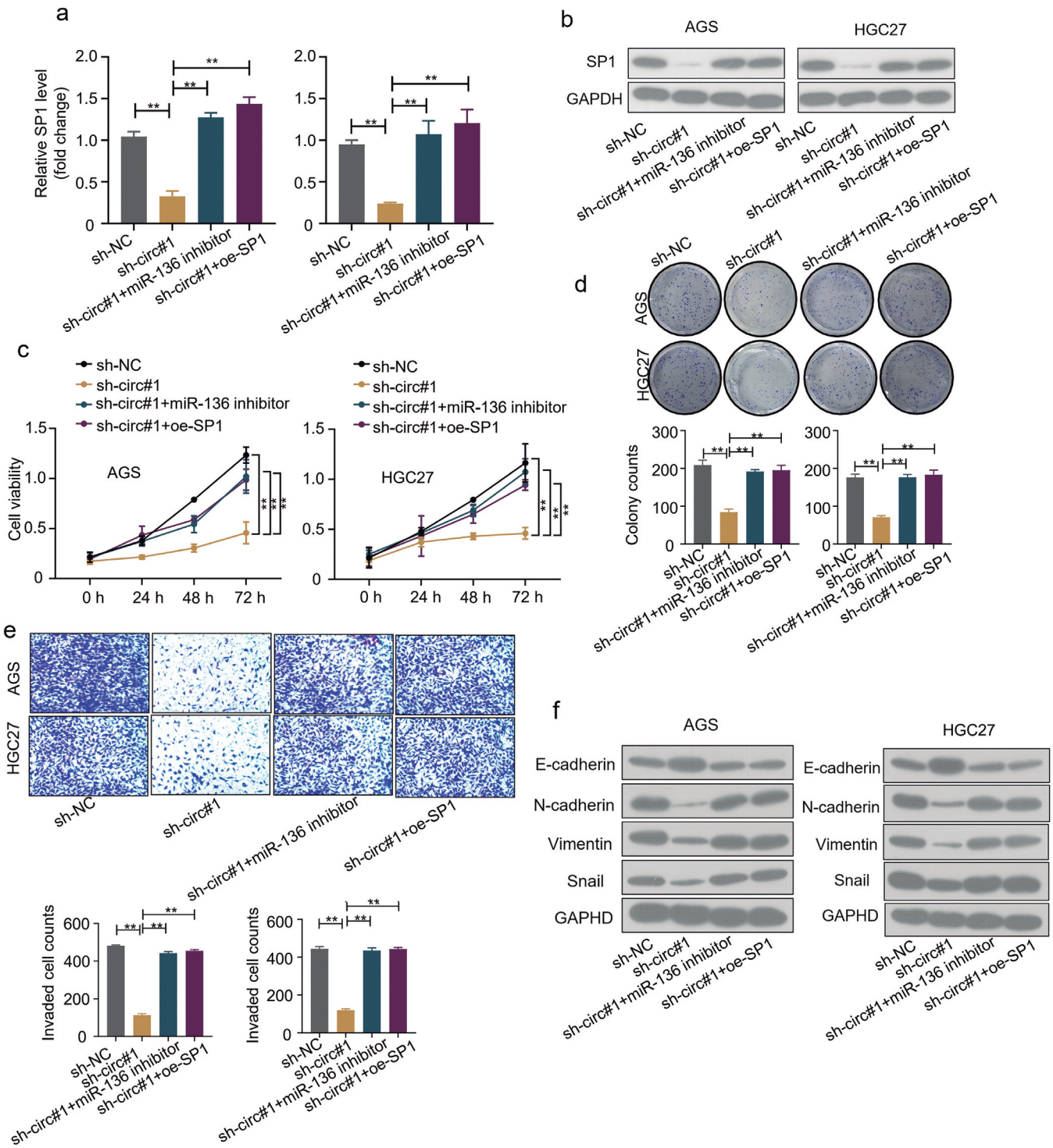

Fig. 6. Circ-0000979 promotes the proliferation and metastasis of gastric carcinoma by sponging miR-136 and modulating SP1. **a.** The SP1 mRNA expression level measured by qRT-PCR after transfection. SP1 mRNA expression was significantly reduced in the circ-0000979-knockdown group compared to the sh-NC control group, while miR-136 inhibition and SP1 overexpression restored the expression. **b.** Western blot analysis revealed that co-transfecting circ-0000979-knockdown GC cell line with miR-136 inhibitor and SP1 overexpression plasmid (oe-SP1) markedly restored the reduced SP1 protein expression level observed after circ-0000979 knockdown. **c.** CCK-8 assay revealed that both miR-136 inhibition and SP1 overexpression significantly increased the viability of GC cell line after circ-0000979 knockdown. **d.** Colony formation assay demonstrated that inhibiting miR-136 and overexpressing SP1 might restore the proliferative ability of GC cell lines. **e.** Transwell assay shows that the migrative ability of the stably silenced circ-0000979 cell lines significantly increased after co-transfection with either miR-136 inhibitor or SP1 overexpression plasmid. **f.** Western blot analysis shows that miR-136 inhibition and SP1 overexpression markedly repressed the E-cadherin protein expression level in the GC cell lines but increased that of N-cadherin, vimentin, and snail. All experiments were performed in triplicate. $^{**}p<0.05$ was chosen as the significant level.

phenotypes, improving the survival rate of patients (Fang et al., 2019). For instance, CiRS-7 was reported to be upregulated in gastric cancer, suppressing the miR-7 function in cancer cells (Pan et al., 2018). CircPVT1, a product of PVT1 gene was found to be up-regulated in GC tissues (Chen et al., 2017) while hsa_circ_0000096 was downregulated in gastric cancer tissues (Li et al., 2017). In the current study, we found that the circ-0000979 is a stable non-coding RNA which is mainly located in the cytoplasm. Consequently, bioinformatics analysis involving differential gene expression revealed that circ-0000979 is highly expressed in gastric tumor tissues and its expression was markedly different when compared with the one observed in normal human gastric epithelial (GSE-1) cells. In addition, the GC patients with high expression of circ-0000979 appeared to show poor prognosis compared with GC patients with low expression, indicating that circ-0000979 promotes the progress and proliferation of GC and might also be a predictive marker for early and precise diagnosis. Importantly, an *in vitro* experiment revealed that silencing of circ-0000979 suppressed GC cell proliferation, migration and invasion capacity by reducing the expression of proliferative proteins (N-cadherin, vimentin, and Snail) while increasing that of E-Cadherin. In the same vein, an *in vivo* study using nude mice revealed that circ-0000979 knockdown significantly reduced tumor formation compared to the control group. Thus, the circ-0000979 might be a potential therapeutic target in treating GC.

To further elucidate the mechanism of action of circ-0000979, we explored the role of miR-136 in association with circ-0000979. Generally, miRNAs have been found to play a crucial role in tumorigenesis. Some miRNAs usually target oncogenes to suppress tumor development, while others function as oncogenes to promote tumor development (Jia et al., 2018). The alteration of miR-136 has been reported in several types of human cancer, including its potential role in carcinogenesis and cancer progression (Chen et al., 2018). For instance, miR-136 serves as a tumor suppressor in Triple Negative Breast Cancer (TNBC) by regulating the RASAL2 gene and modulating the Mesenchymal to Epithelial Transition (MET) (Yan et al., 2016), its expression depreciated in hepatocellular carcinoma tissues and cells, and was negatively correlated with COX2 mRNA expression (Jia et al., 2018). Contrarily, a report shows that miR-136 is markedly upregulated in human non-small-cell lung cancer (NSCLC) primary tumors and cell lines when compared to their non-tumor counterparts and promotes the proliferation of the cell (Shen et al., 2014). In order to further elucidate on the mechanism through which circ-0000979 regulates the progression of GC cell, the precise mechanisms underlying induced inhibitory outcome of miR-136 were elucidated using the bioinformatics prediction analysis and confirmed through a dual-luciferase reporter assay and biotinylated RNA-Pulldown assay. Also, qRT-PCR analysis shows that miR-136 was sufficiently upregulated in the absence of circ-0000979 in GC tissues indicating that the expression of miR-136 is negatively correlated with circ-0000979. Bioinformatics prediction also indicated that the 3'UTR region of SP1 is a target for miR-136. SP1 is a transcription factor protein that mediates the maintenance of normal and cancerous biological processes (Vellingiri et al., 2020). Subsequently, luciferase reporter assay showed that miR-136 overexpression markedly depreciates the luciferase activity of cells under the influence of SP1 wild type plasmid. This effect showed no significant difference with the mutant type plasmid. Surprisingly, the expression of SP1 mRNA significantly increased after the inhibition of miR-136 in the GC cell lines, indicating that miR-136 was able to bind to the 3'UTR region of SP1 mRNA and repress its protein expression level. Put together, these outcomes suggest that miR-136 may play the role of a tumor suppressor by regulating the SP1 expression level in GC tissues.

Epithelial Mesenchymal Transition (EMT) pathway has been implicated in tumorigenesis by promoting metastasis, chemoresistance and tumor stemness as well as acting as a potent driver of tumors. Upregulation of N-cadherin, as well as the downregulation of E-Cadherin, signifies the hallmark of EMT, a process that is associated with regulated complex signaling pathways and transcription (Loh et al., 2019). High expression of E-Cadherin and downregulation of N-Cadherin was associated with increased apoptosis, weaker invasiveness and low adhesion to extracellular matrix (ECM) in ovarian cancer (Rosso et al., 2017) and its abnormal expression significantly correlated with tumor stage in gastric cancer patients (Torabizadeh et al., 2017). In this investigation, qRT-PCR analysis showed that silencing circ-0000979 correlates strongly with low expression of SP1, whereas miR-136 inhibitor significantly increased the expression of SP1. Also, silencing circ-0000979 reduces cell viability in gastric cancer, whereas cell viability rebounds partially in the presence of miR-136 inhibitor. Besides, silencing circ-0000979 led to a significant depreciation of cell proliferation, invasion, and migration in GC tissues. In the same vein, western blot analysis revealed that silencing circ-0000979 effectively increased the level of anti-proliferative protein E-cadherin while reducing the expression level of proliferative protein N-cadherin and Vimentin. Interestingly, upon transfection with miR-136 inhibitor or SP1 overexpression plasmid, the expression level of the proliferative proteins was restored. Taken together, the results from this investigation suggest that circ-0000979 promotes the progress of gastric cancer via the miR-136/SP1 pathway. Although our results validated the role of circ-0000979 in GC, the aggressiveness and heterogeneous nature of the disease (Gao et al., 2018) calls for a follow-up study to confirm the role of the reported biological molecules in higher sample numbers. Also, examining the role of these molecules in GC patients under different environment factors would

provide valuable information needed for the development of effective therapeutic drug target for treating different GC patients.

In summary, circ-0000979 is an oncogenic circRNA that promotes the progression of gastric cancer by regulating the miR-136/SP1 pathway. Circ-0000979 might be an RNA therapeutic target for gastric cancer treatment.

Acknowledgements. Not applicable.

Declaration of interest. The authors declare that they have no conflict of interest.

Authors' contributions. Lei Bao designed the project, collected data, analyzed the data and drafted the manuscript. Lihua Zhang did almost all the experiments, and Fengjuan Xing did some experiments and were involved in data collection and analysis. All the authors revised and corrected the manuscript.

Funding. No funding.

Availability of data and materials. The datasets used and/or analysed during the current study are available from the corresponding author on reasonable request.

References

Bi W., Huang J., Nie C., Liu B., He G., Han J., Pang R., Ding Z., Xu J. and Zhang J. (2018). CircRNA CircRNA_102171 promotes papillary thyroid cancer progression through modulating CTNNBIP1-dependent activation of β-catenin pathway. J. Exp. Clin. Cancer Res. 37, 275.

Bray F., Ferlay J., Soerjomataram I., Siegel R.L., Torre L.A. and Jemal A. (2018). Global cancer statistics 2018: GLOBOCAN estimates of incidence and mortality worldwide for 36 cancers in 185 countries. CA Cancer J. Clin. 68, 394-424.

Chen J., Li Y., Zheng Q., Bao C., He J., Chen B., Lyu D., Zheng B., Xu Y., Long Z., Zhou Y., Zhu H., Wang Y., He X., Shi Y. and Huang S. (2017). Circular RNA profile identifies circPVT1 as a proliferative factor and prognostic marker in gastric cancer. Cancer Lett. 388, 208-219.

Chen X., Huang Z. and Chen R. (2018). MicroRNA-136 promotes proliferation and invasion ingastric cancer cells through Pten/Akt/P-Akt signaling pathway. Oncol. Lett. 15, 4683-4689.

Cho J.H., Jeon S.R. and Jin S.Y. (2020). Clinical applicability of gastroscopy with narrow-band imaging for the diagnosis of Helicobacter pylori Gastritis, precancerous gastric lesion, and Neoplasia. World J. Clin. Cases 8, 2902-2916.

D'Angelica M., Gonen M., Brennan M.F., Turnbull A.D., Bains M. and Karpeh M.S. (2004). Patterns of Initial recurrence in completely resected gastric adenocarcinoma. Ann. Surg. 240, 808-816.

Fang X., Wen J., Sun M., Yuan Y., Xu Q. (2019). CircRNAs and its relationship with gastric cancer. J. Cancer 10, 6105-6113.

Gao J.P., Xu W., Liu W.T., Yan M. and Zhu Z.G. (2018). Tumor heterogeneity of gastric cancer: From the perspective of tumor-initiating cell. World J. Gastroenterol. 24, 2567-2581.

Jia H., Wang H., Yao Y., Wang C. and Li P. (2018). MiR-136 inhibits malignant progression of hepatocellular carcinoma cells by targeting cyclooxygenase 2. Oncol. Res. 26, 967-976.

Jin J., Chen A., Qiu W., Chen Y., Li Q., Zhou X. and Jin D. (2019). Dysregulated CircRNA_100876 suppresses proliferation of osteosarcoma cancer cells by targeting microRNA-136. J. Cell. Biochem. 120, 15678-15687.

Katai H., Ishikawa T., Akazawa K., Isobe Y., Miyashiro I., Oda I., Tsujitani S., Ono H., Tanabe S., Fukagawa T., Nunobe S., Kakeji Y., Nashimoto A. and A Registration Committee of the Japanese Gastric Cancer (2018). Five-year survival analysis of surgically resected gastric cancer cases in Japan: A retrospective analysis of more than 100,000 patients from the nationwide registry of the Japanese gastric cancer association (2001-2007). Gastric Cancer 21, 144-154.

Li P., Chen H., Chen S., Mo X., Li T., Xiao B., Yu R. and Guo J. (2017). Circular RNA 0000096 affects cell growth and migration in gastric cancer. Br. J. Cancer 116, 626-633.

Li R., Jiang J., Shi H., Qian H., Zhang X. and Xu W. (2020). CircRNA: A rising star in gastric cancer. Cell Mol. Life Sci. 77, 1661-1680.

Loh C.Y., Chai J.Y., Tang T.F., Wong W.F., Sethi G., Shanmugam M.K., Chong P.P. and Looi C.Y. (2019). The E-Cadherin and N-Cadherin switch in epithelial-to-mesenchymal transition: Signaling, therapeutic implications, and challenges. Cells 8, 1118.

Machlowska J., Baj J., Sitarz M., Maciejewski R. and Sitarz R. (2020). Gastric cancer: Epidemiology, risk factors, classification, genomic characteristics and treatment strategies. Int. J. Mol. Sci. 21, 4012.

Martin-Richard M., Carmona-Bayonas A., Custodio A.B., Gallego J., Jimenez-Fonseca P., Reina J.J., Richart P., Rivera F., Alsina M. and Sastre J. (2020). SEOM clinical guideline for the diagnosis and treatment of gastric cancer (GC) and gastroesophageal junction adenocarcinoma (GEJA) (2019). Clin. Transl. Oncol. 22, 236-244.

Pan H., Li T., Jiang Y., Pan C., Ding Y., Huang Z., Yu H. and Kong D. (2018). Overexpression of circular RNA ciRS-7 abrogates the tumor suppressive effect of miR-7 on gastric cancer via PTEN/PI3K/AKT signaling pathway. J. Cell Biochem. 119, 440-446.

Peng F., Gong W., Li S., Yin B., Zhao C., Liu W., Chen X., Luo C., Huang Q., Chen T., Sun L., Fang S., Zhou W., Li Z. and Long H. (2020). circRNA_010383 acts as a sponge for miR-135a and its downregulated expression contributes to renal fibrosis in diabetic nephropathy. Diabetes 70, 603-615.

Qu Y., Dou P., Hu M., Xu J., Xia W. and Sun H. (2019). circRNA-CER mediates malignant progression of breast cancer through targeting the miR-136/MMP13 axis. Mol. Med. Rep. 19, 3314-3320.

Rawla P. and Barsouk A. (2019). Epidemiology of gastric cancer: Global trends, risk factors and prevention. Prz. Gastroenterol. 14, 26-38.

Rosso M., Majem B., Devis L., Lapyckyj L., Besso M.J., Llaurado M., Abascal M.F., Matos M.L., Lanau L., Castellvi J., Sanchez J.L., Perez Benavente A., Gil-Moreno A., Reventos J., Santamaria Margalef A., Rigau M. and Vazquez-Levin M.H. (2017). E-Cadherin: A determinant molecule associated with ovarian cancer progression, dissemination and aggressiveness. PLoS One 12, e0184439.

Shen S., Yue H., Li Y., Qin J., Li K., Liu Y. and Wang J. (2014). Upregulation of miR-136 in human non-small cell lung cancer cells promotes Erk1/2 activation by targeting PPP2R2A. Tumour Biol. 35, 631-640.

Shi S. and Zhang Z.G. (2019). Role of Sp1 expression in gastric cancer: A meta-analysis and bioinformatics analysis. Oncol. Lett. 18, 4126-4135.

Sitarz R., Skierucha M., Mielko J., Offerhaus G.J.A., Maciejewski R. and Polkowski W.P. (2018). Gastric cancer: Epidemiology, prevention, classification, and treatment. Cancer Manag. Res. 10, 239-248.

Suzuki H. and Tsukahara T. (2014). A view of pre-mRNA splicing from RNase R resistant RNAs. Int. J. Mol. Sci. 15, 9331-9342.

Tang W., Fu K., Sun H., Rong D., Wang H. and Cao H. (2018). CircRNA microarray profiling identifies a novel circulating biomarker for detection of gastric cancer. Mol. Cancer 17, 137.

Tian Y., Ma R., Sun Y., Liu H., Zhang H., Sun Y., Liu L., Li Y., Song L. and Gao P. (2020). Sp1-activated Long noncoding RNA lncRNA GCMA functions as a competing endogenous RNA to ppromote tumor metastasis by sponging miR-124 and miR-34a in gastric cancer. Oncogene 39, 4854-4868.

Torabizadeh Z., Nosrati A., Sajadi Saravi S.N., Yazdani Charati J. and Janbabai G. (2017). Evaluation of E-cadherin expression in gastric cancer and its correlation with clinicopathologic parameters. Int. J. Hematol. Oncol. Stem Cell Res. 11,158-164.

Vellingiri B., Iyer M., Subramaniam M.D., Jayaramayya K., Siama Z., Giridharan B., Narayanasamy A., Dayem A.A. and Cho S.G. (2020) Understanding the role of the transcription factor Sp1 in ovarian cancer: From theory to practice. Int. J. Mol. Sci. 21, 1153.

Yan M., Li X., Tong D., Han C., Zhao R., He Y. and Jin X. (2016). MiR-136 suppresses tumor invasion and metastasis by targeting RASAL2 in triple-negative breast cancer. Oncol. Rep. 36, 65-71.

Yu L., Zhou G.Q. and Li D.C. (2018). MiR-136 triggers apoptosis in human gastric cancer cells by targeting AEG-1 and BCL2. Eur. Rev. Med. Pharmacol. Sci. 22, 7251-7256.

Zang D., Zhang C., Li C., Fan Y., Li Z., Hou K., Che X., Liu Y. and Qu X. (2020). LPPR4 promotes peritoneal metastasis via Sp1/integrin α/FAK signaling in gastric cancer. Am. J. Cancer Res. 10, 1026-1044.

Zhang X., Tan P., Zhuang Y. and Du L. (2020). hsa_CircRNA_001587 upregulates SLC4A4 expression to inhibit migration, invasion, and angiogenesis of pancreatic cancer cells via binding to microRNA-223. Am. J. Physiol. Gastrointest. Liver Physiol. 319, G703-G17.

Zheng J., Ge P., Liu X., Wei J., Wu G. and Li X. (2017) MiR-136 inhibits gastric cancer-specific peritoneal metastasis by targeting HOXC10. Tumour Biol. 39, 1010428317706207.

Zhu J., Wang S.M., Chen R., Li X.Q. and Wei W.W. (2020). Progress on screening for gastric cancer. Chinese J. Oncol. 42, 603-608.

Zong L., Sun Q., Zhang H., Chen Z., Deng Y., Li D. and Zhang L. (2018). Increased expression of CircRNA_102231 in lung cancer and its clinical significance. Biomed. Pharmacother. 102, 639-644.

Accepted December 21, 2022